

# The $\beta$ – $\alpha$ Branching in D-Sorbitol as Studied by Thermally Stimulated Depolarization Currents (TSDC)

Nátalia T. Correia, Cristina Alvarez, and Joaquim J. Moura Ramos\*

Centro de Química-Física Molecular, Complexo I, IST, Avenida Rovisco Pais, 1049-001 Lisboa, Portugal

Marc Descamps\*

Laboratoire de Dynamique et Structure des Matériaux Moléculaires, UFR Physique, Bâtiment P5, 59655 Villeneuve d'Ascq Cedex, France

Received: December 7, 2000; In Final Form: March 26, 2001

The molecular motions in D-sorbitol (D-glucitol) have been studied by thermally stimulated depolarization currents (TSDC) in the temperature region between  $-160$  and  $10$  °C. The  $\beta$  relaxation appears as a broad global peak between  $-160$  and  $-50$  °C and its features were compared with those of the  $\beta$  relaxation of maltitol (a D-glucitol derivative). A study of the  $\alpha$  relaxation of sorbitol, which shows a maximum intensity at approximately  $-1$  °C, is also presented, and from the obtained data, the fragility index of this glass former is calculated. The  $\alpha$  and  $\beta$  relaxations are observed to merge in the frequency window of the TSDC technique, and it is underlined that this merging is a consequence of the overlap of the tails of these distributions in this frequency window. In this context, the merging observed by TSDC images the branching of the most probable times of the two distributions predicted by dielectric relaxation spectroscopy at the branching temperature  $T_{\alpha\beta}$ .

## Introduction

In recent works, we have used the technique of thermally stimulated depolarization currents (TSDC) to study the relaxation mechanisms present in several liquid-crystalline polymers<sup>1,2</sup> and molecular glass formers, namely, glycerol, salol, maltitol, and *m*-toluidine.<sup>3,4</sup> In this context, we showed<sup>2,3</sup> that it is possible to use TSDC data obtained on the  $\alpha$  relaxation of this glass formers to obtain the fragility index, a fundamental parameter in glassy state physics that is at the center of glass relaxational behavior.

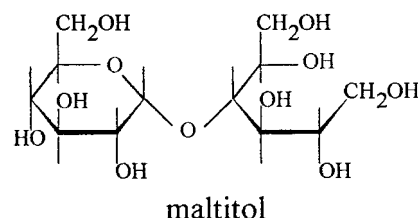
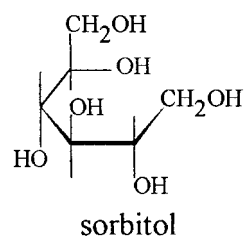
An important advantage of the TSDC technique is the possibility of experimentally resolving a broad global relaxation into its different individual components, fractions, or segments, i.e., the possibility of separating a broad distribution of relaxations into its narrowly distributed components (see Experimental Section). This allows, as will be seen later, different components of a given relaxation (central components of the distribution of relaxation times, as well as queues or tails of this distribution) to be determined.

In the present work, we report the results obtained on another glass former, D-sorbitol. From dielectric studies, it was shown that D-sorbitol presents a very pronounced  $\beta$ -relaxation process.<sup>5,6</sup> On the other hand, it constitutes a representative example of a material in which the  $\beta$  process is observed in the metastable supercooled liquid state by dielectric relaxation spectroscopy (DRS) and then merges into the  $\alpha$  relaxation.<sup>6–8</sup> This glass former thus appears to be an excellent system for a TSDC investigation of the branching between the main and the secondary processes. We first present a detailed explanation of the physical significance of the results provided by the TSDC technique. In this context, it is shown that TSDC provides very

useful information on the distribution of relaxation times of a given relaxation. A full TSDC analysis of the  $\beta$  relaxation of sorbitol is then presented. The width of this relaxation, its structure, and the extension of the overlap between the  $\beta$  and  $\alpha$  relaxations are discussed in comparison with the TSDC data obtained for the glass former maltitol. Finally, a discussion of  $\alpha$  relaxation is presented, and the fragility index of sorbitol is estimated from TSDC data.

## Experimental Section

D-Sorbitol ( $C_6H_{14}O_6$ , D-glucitol) was an Aldrich product with a purity of  $>99\%$  (catalog no. 24,085,0) and a melting point at  $106$  °C, and it was used without further purification. Its calorimetric glass transition temperature is reported to be  $T_g = -1.3$  °C ( $271.8$  K).<sup>9,10</sup>



\* Authors for correspondence. Moura Ramos: e-mail mouraramos@ist.utl.pt, fax 351-21-846 44 55. Descamps: e-mail Marc.Descamps@univ-lille1.fr, fax 00-33-3-20434084.

Thermally stimulated depolarization current (TSDC) experiments were carried out with a TSC/RMA spectrometer (Solomat

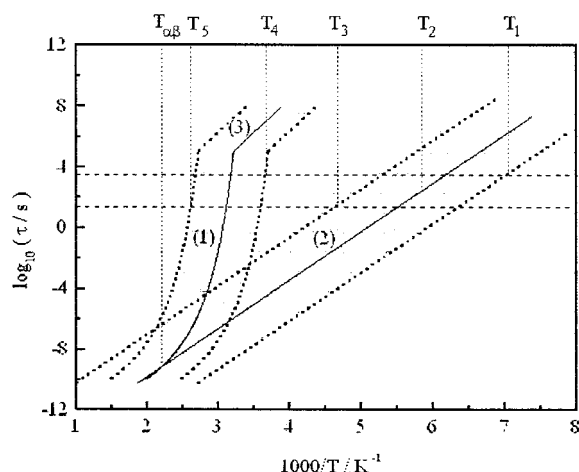


**Figure 1.** Schematic representation of a typical relaxation map for the  $\alpha$  and  $\beta$  relaxation processes. Line 1 corresponds to the  $\alpha$  relaxation, line 2 to the  $\beta$  relaxation, and line 3 to the so-called return to Arrhenius (motions in the frozen, nonannealed glass). The horizontal dashed lines correspond to the higher and lower limits of the relaxation times probed by the TSDC technique. The dotted lines schematically represent the width of the distribution of relaxation times associated with each distribution. The temperature  $T_{\alpha\beta}$  corresponds to the branching position of the most probable times,  $\langle\tau_{\alpha}\rangle$  and  $\langle\tau_{\beta}\rangle$ , of the  $\alpha$  and  $\beta$  relaxations, respectively.

Instruments, Stamford, CT) covering the range  $-170$  to  $+400$  °C. To analyze specific regions of the TSDC spectrum, different methods of polarizing the sample were used, namely, the so-called TSDC global experiment and the thermal sampling (TS) experiment (often called thermal windowing or cleaning). The physical foundations of the TSDC technique and the nature of the information that it provides have been addressed several times in recent publications,<sup>2–4</sup> so we avoid unnecessary repetition here. The technique of TS allows a complex relaxation to be resolved into its individual relaxation modes. A very specific feature of the TSDC technique is that it allows for the determination of different components of the distribution of relaxation times of a given relaxation, and not only the most probable time. The TS experiments are thus performed in order to study the detail of each complex relaxation [distributions of the energy (or enthalpy) and/or of the preexponential factor (or entropy)]. Readers who are not familiar with the TSDC technique and data treatment can find useful information about this subject elsewhere.<sup>3,11–13</sup>

**The TSDC Technique as a Probe of Slow Relaxations.** The TSDC technique probes slow molecular motions, so it is equivalent to a low-frequency technique (it probes a time window between 25 and 3000 s, which corresponds to a frequency window between  $5 \times 10^{-5}$  and  $6 \times 10^{-3}$  Hz).

Figure 1 shows a representation of a typical relaxation map for a glass forming system with  $\alpha$  and  $\beta$  relaxations. Line 1 in Figure 1 represents a Vogel-type line that is a feature of the glass transition relaxation, whereas line 2 represents a typical  $\log \tau$  versus  $1/T$  line for a secondary relaxation. The horizontal dashed lines indicate the higher and lower limits of the relaxation times probed by the TSDC technique. In the following paragraphs, we try to situate the contribution of TSDC to the study of molecular mobility in the context of the relaxation map shown in Figure 1.

Recall that the  $\alpha$  and  $\beta$  relaxations correspond not to single or elementary motions, but rather to a distribution of motions, thus presenting a distribution of relaxation times. The dotted lines in Figure 1 represent the width of the distribution of relaxation times associated with each distribution. If a TS

experiment is carried out with a polarization temperature,  $T_P$ , lower than  $T_1$  in Figure 1, no polarization is frozen-in, and no TS peak is obtained. However, if the polarization temperature of the TS experiment is  $T_1$ , the polarizing field is able to pick up the shorter times of the distribution of relaxation times of the  $\beta$  relaxation. For TS experiments with  $T_P$  between  $T_1$  and  $T_3$ , the electric field polarizes the different components of the secondary relaxation. For example, for  $T_P \approx T_2$ , the most probable time of the distribution is polarized, and for  $T_P = T_3$ , the longer times of the distribution are polarized. The TSDC technique thus probes the longer times of the distribution at high temperatures and the shorter times at low temperatures. Between  $T_3$  and  $T_4$ , there are no molecular motions with characteristic times observable within the range of the TSDC window. Between  $T_4$  and  $T_5$ , the electric field polarizes the different components of the  $\alpha$  relaxation. As is shown later, no TS peaks are obtained between  $T_g$  and  $T_5$ , because the equilibration processes are very fast in this temperature range, preventing the freezing-in of the polarization.

Figure 1 underlines some important features of the TSDC technique. One is that, as a consequence of its low activation energy, the  $\beta$  relaxation appears in the TSDC spectrum as a broad relaxation that is observed in a large temperature interval (between  $T_1$  and  $T_3$ ), when compared with the  $\alpha$  relaxation (which appears in Figure 1 between  $T_4$  and  $T_5$ ). Another feature that is underlined in Figure 1, and is very specific to this experimental technique, is that it allows for the determination of different components of the distribution of relaxation times of a given relaxation, and not only the most probable time. This will be illustrated in the next section.

The output of a TSDC experiment is a peak of the depolarization current intensity as a function of temperature. These TSDC peaks have different characteristics for the  $\alpha$  and  $\beta$  relaxations. In fact, the TSDC global peak of the  $\beta$  relaxation is much broader than that of the  $\alpha$  relaxation (see bottom of Figure 2). Moreover, the shape of the TS peaks is also different for the  $\alpha$  and  $\beta$  relaxations. For the  $\alpha$  relaxation, the TS peaks are asymmetrical, showing a gradual increase followed by a sharp decrease in the current intensity (as shown at the bottom of Figure 2a). This shape can be understood examining Figure 2a and b (top), which represents the amount of polarization created at each polarization temperature,  $T_P$ , in the same polarization time,  $t_P$ , (continuous line) and the amount of polarization lost in the thermal treatment after removal of the polarizing field (dotted line).

The vertical distance between the two lines represents the polarization that is frozen-in in each experiment (with a given polarization temperature) and that will depolarize during the heating ramp (with constant heating rate) of the experiment, giving rise to the TSDC peak. For the TS peak with maximum intensity in the glass transition region (the peak with maximum intensity at  $T_M$ ), this distance is a maximum (see Figure 2a). Above  $T_M$ , the depolarization becomes very rapid, preventing retention of the polarization. That is why the intensities of the maxima of the TS peaks above  $T_M$  in the glass transition region decrease sharply as  $T_P$  increases (dashed peaks at the bottom of Figure 2a; see also dashed peaks in Figure 6). This is also why the TS peaks in the glass transition region exhibit a sharp decrease of the current intensity (a fast depolarization) above the temperature of maximum intensity. Above  $T_M$ , the freezing-in of the polarization is increasingly difficult, indicating a transformation to the equilibrium (ergodic) metastable supercooled liquid state. Thus, the temperature,  $T_M$ , of the TS peak with higher intensity in the glass transition region probably

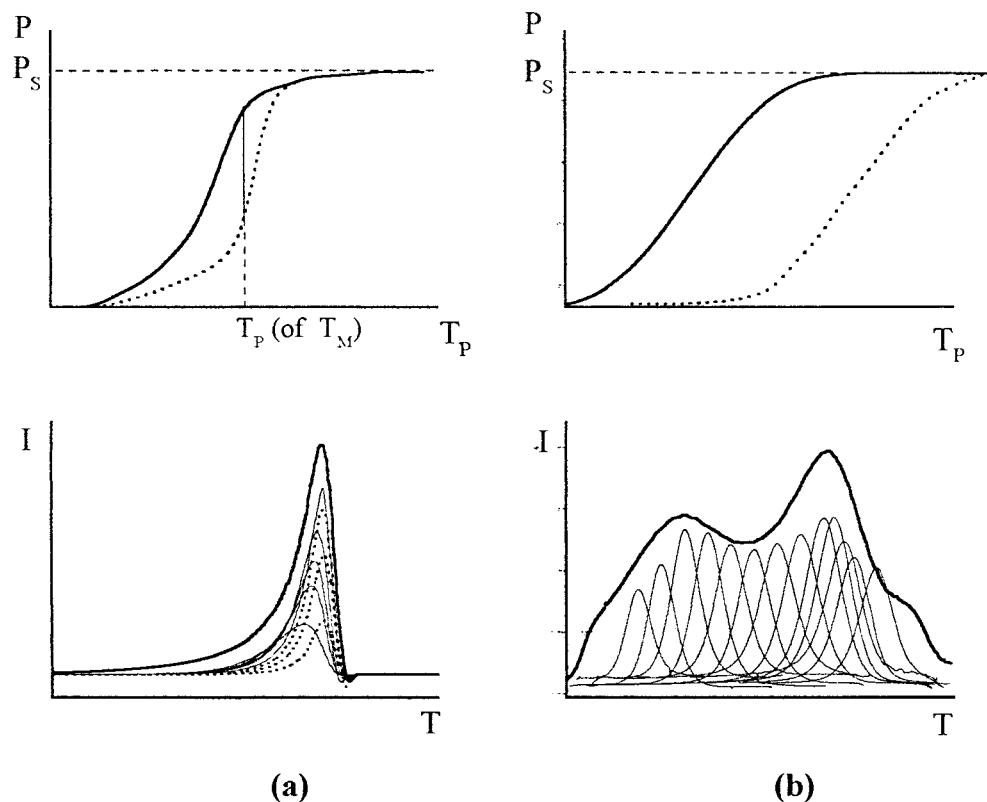


**Figure 2.** Amount of polarization,  $P$ , created at each polarization temperature,  $T_p$ , in the same polarization time,  $t_p$ , (continuous line) and the amount of polarization lost in the thermal treatment after the removal of the polarizing field (dotted line).  $P_s$  is the saturation polarization. The vertical distance between the two lines represents the polarization that was frozen-in in each experiment (with a given polarization temperature). Plot a corresponds to the glass transition relaxation, whereas the plot b corresponds to the  $\beta$  relaxation. At the bottom of the figure are shown experimental results (TSDC peaks) corresponding to situations a and b. The thicker lines are global relaxation peaks, and the thin ones are TS peaks.

represents the lower-temperature limit of the transformation range, defining a time scale of the system when nearly all of the activation barriers are activated (a time scale of the system very near the equilibrium). Figure 2b, on the other hand, corresponds to a broad relaxation, as is the case for the  $\beta$  relaxation observed by TSDC. The relaxation now spans a large temperature interval, the TSDC global peak is very broad, and the corresponding TS peaks do not show the asymmetry that is a feature of the TS peaks in the glass transition region.

## Results and Discussion

Two relaxation mechanisms were detected in the TSDC study of sorbitol: a higher intensity one, with a maximum intensity at approximately  $-1$  °C, that is the glass transition relaxation or  $\alpha$  relaxation, and a broad and lower-intensity one, spread over the temperature range between  $-160$  and  $-50$  °C, that is the  $\beta$  relaxation. In the following, we report the results obtained in the study of each of these relaxations.

**$\beta$  Relaxation and  $\beta$ - $\alpha$  Merging.** Figure 3 shows the results of two TSDC global experiments obtained with the polarizing field applied in the temperature region of the  $\beta$  relaxation. The broadness of this global peak and its irregular profile suggest that it corresponds to a complex process, involving relaxation mechanisms occurring in a variety of environments.

It is to be noted that the increase observed on the right-hand side of the dashed curve in Figure 3 corresponds to the beginning of the  $\alpha$  relaxation and indicates the strong overlap that exists between the primary and secondary relaxations in sorbitol.

Figure 4 shows the experimental decomposition of this broad relaxation into its thermal sampling (TS) components.

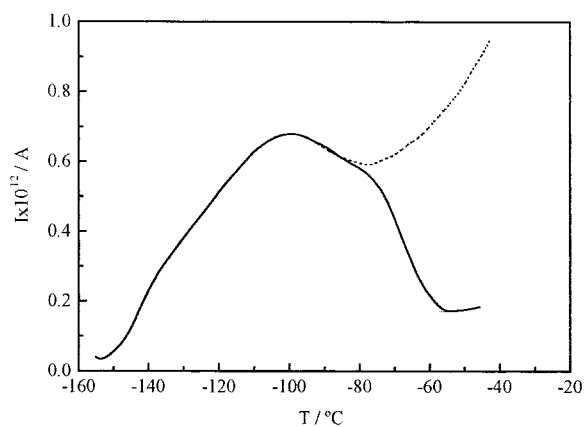


**Figure 3.** Two TSDC global peaks in the region of the  $\beta$  relaxation of sorbitol. The temperature range where the polarizing field was applied included polarization temperatures,  $T_p = -80$  °C (solid curve),  $T_p = -30$  °C (dotted curve), and freezing temperature  $T_0 = -155$  °C. The strength of the polarizing electric field was  $E = 100$  V/mm, the polarization time was 5 min, and the rate of the heating ramp was 8 °C/min.

The increasing intensity of the TS peaks on the right-hand side of Figure 4 indicates again that, for temperatures above  $-60$  °C, the  $\beta$  relaxation merges with the  $\alpha$  relaxation. This behavior was not observed in our previous TSDC study of maltitol,<sup>3</sup> where both relaxations appeared well separated. The  $\alpha$ - $\beta$  merging is thus clearly observed in sorbitol, within the time window of the TSDC technique.

The  $\log \tau(T)$  versus  $1/T$  lines of the TS peaks of the  $\beta$  relaxation were obtained, as usual,<sup>14</sup> by the Bucci method.<sup>15,16</sup>

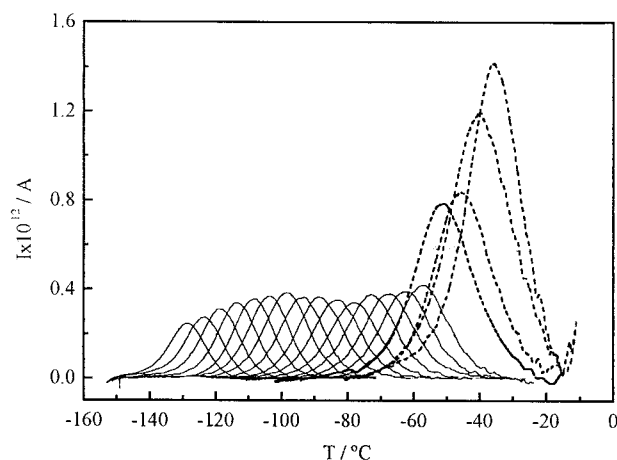


**Figure 4.** TS components of the  $\beta$  relaxation of sorbitol. The polarization temperatures varied between  $-135$  and  $-45$   $^{\circ}\text{C}$ , with intervals of  $5$   $^{\circ}\text{C}$ . The strength of the polarizing electric field was  $E = 200$  V/mm, the polarization time was  $5$  min, the width of the polarization window was  $2$   $^{\circ}\text{C}$ , and the heating rate was  $4$   $^{\circ}\text{C min}^{-1}$ . The dashed peaks, which show increasing intensity, correspond to the merging of the two relaxations.

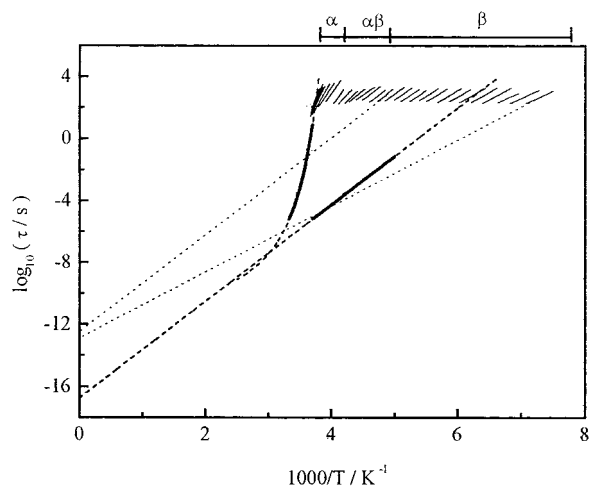


**Figure 5.** Relaxation map for the  $\alpha$  and  $\beta$  relaxations of sorbitol. The thicker lines describe the temperature evolution of the most probable relaxation time and were obtained from dielectric relaxation spectroscopy.<sup>6</sup> The smaller and thinner lines are the  $\log \tau_{\beta}(T)$  versus  $1/T$  lines of the thermally sampled components of the  $\alpha$  and  $\beta$  relaxations of sorbitol obtained by TSDC. The dotted lines are just guides to the eye, and they give a visual indication of the order of magnitude of the preexponential factor of the TS components of the  $\beta$  process obtained by the fitting.

Figure 5 shows the relaxation map of sorbitol and includes the temperature evolution of the most probable relaxation time obtained by dielectric relaxation spectroscopy for the  $\alpha$  and  $\beta$  relaxations,<sup>6</sup> as well as the  $\log \tau(T)$  versus  $1/T$  lines of the TS components of these two relaxations.

The dotted lines in Figure 5 delimit the TS lines that belong to the  $\beta$  relaxation and indicate the order of magnitude of the preexponential factors obtained from the fittings. The dashed lines in Figure 5 are just extrapolations of the dielectric relaxation data.

The activation parameters of the TS components of the  $\beta$  relaxation (and of the  $\alpha$  relaxation) were obtained from the fitting of their  $\log \tau(T)$  versus  $1/T$  lines. The activation enthalpies of the TS components are represented in Figure 6 (circles) as a function of their location on the temperature axis,  $T_m$ . The results obtained in the TSDC study of the glass former maltitol<sup>3</sup> are also shown for comparison (triangles).

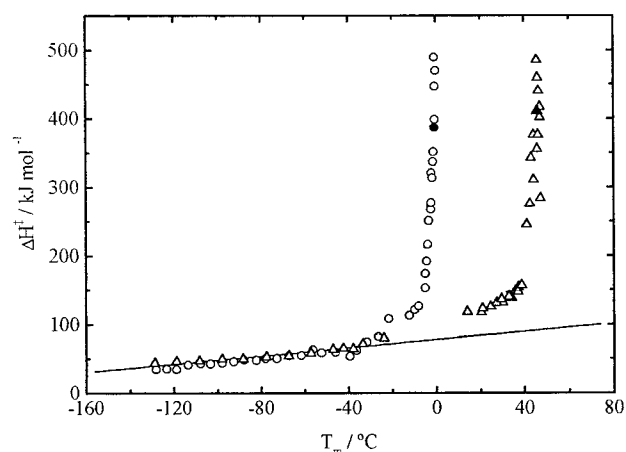


**Figure 6.** Activation enthalpy of the TS components of the  $\beta$  and  $\alpha$  relaxations of sorbitol (O) and maltitol ( $\Delta$ ) as functions of the peak's location,  $T_m$ . The continuous line corresponds to the zero-entropy prediction. The full symbols correspond to the TS peak with higher intensity in the glass transition region.

The continuous line in Figure 6 is the so-called zero-entropy line that depicts the behavior expected for noncooperative relaxations (see refs 3 and 4 about the significance of the zero-entropy line). It can be seen that the lower-temperature TS components (those of the  $\beta$  relaxation) show a zero-entropy behavior. As a consequence, they show activation enthalpies that slightly increase with increasing temperature. As an illustration, in the present case of sorbitol, the TS component at  $T_m = -128$   $^{\circ}\text{C}$  (obtained with a polarization temperature of  $T_p = -135$   $^{\circ}\text{C}$ ) has an activation enthalpy of  $37$   $\text{kJ mol}^{-1}$ , whereas the TS component at  $T_m = -56.4$   $^{\circ}\text{C}$  (obtained with a polarization temperature of  $T_p = -65$   $^{\circ}\text{C}$ ) has an activation enthalpy of  $70$   $\text{kJ mol}^{-1}$ . These low-temperature components of the  $\beta$  relaxation, which show low activation enthalpies and no activation entropy, thus correspond to local and noncooperative motions.<sup>6,17,18</sup> The values reported in the literature for the Arrhenius activation energy of the  $\beta$  relaxation of sorbitol, obtained by dielectric relaxation spectroscopy, are  $55.3$ ,<sup>18</sup>  $59.8$ ,<sup>6</sup> and  $61.4$   $\text{kJ mol}^{-1}$ .<sup>5</sup> It is to be noted that these values are within the energy interval previously reported for the activation enthalpies of the TS components of the  $\beta$  relaxation. Note that the information regarding the  $\beta$  relaxation shown in Figures 5 and 6 is equivalent. In fact, Figure 5 suggests a similar prefactor, on the order of  $10^{-13}$  s, for the TS lines of the  $\beta$  relaxation, which is equivalent to saying that the corresponding motions have no activation entropy, as shown in Figure 6.

Figure 6 also shows that, at low temperatures, the activation energies are similar for sorbitol and maltitol, in agreement with the dielectric results. The TSDC data thus confirm that the temperature evolution of the mean relaxation times of the  $\beta$  relaxation is identical for sorbitol and maltitol.<sup>5</sup> Moreover, in the case of sorbitol, there is no discontinuity or gap in Figure 6 between the TS components of the  $\beta$  process and those of the  $\alpha$  process, indicating the overlap of the two processes. From Figure 6, it is also apparent that this overlap between the  $\beta$  and  $\alpha$  relaxations is not observed in the case of maltitol. In fact, the gap between  $-20$  and  $10$   $^{\circ}\text{C}$  observed in Figure 6 for the data relative to maltitol (triangles) arises from the fact that the polarizing electric field is not able to create any appreciable polarization in this temperature region (no TS peaks with significant intensity are obtained when the polarization temperature,  $T_p$ , is higher than  $-27$   $^{\circ}\text{C}$  and lower than  $5$   $^{\circ}\text{C}$ ). This corresponds to the situation described in Figure 1 between  $T_3$  and  $T_4$ . Note that the merging between the  $\beta$  and  $\alpha$  relaxations



appears in the TSDC technique as an overlap of the wings of the distributions of the two relaxations. Otherwise stated, in the frequency window of the TSDC technique, the higher-temperature components of the  $\beta$  relaxation and the lower-temperature components of the  $\alpha$  relaxation appear in the same temperature region, as shown in Figure 5.

The structural difference between maltitol and sorbitol is the presence, in maltitol, of a bulky substituent (a six-membered heterocycle) that substitutes the hydroxylic hydrogen in position 3. This is probably the reason the glass transition temperature is higher in maltitol than in sorbitol, suggesting that this bulky substituent has a hindering effect on the cooperative motions associated with the glass transition. On the other hand, the fact that the  $\beta$  relaxations in maltitol and sorbitol are superposed suggests that the local internal rotations and librations are probably affected to a lesser extent by the presence of the bulky group. That is why the  $\alpha$  and  $\beta$  relaxations appear reasonably well separated in maltitol, whereas they strongly overlap in sorbitol, as shown in Figures 5 and 6. This indicates that the bifurcation of the  $\alpha$  and  $\beta$  processes occurs for different frequencies in maltitol and sorbitol and that, for sorbitol, it occurs closer to the frequency window of the TSDC technique. The mean relaxation times of the  $\alpha$  process,  $\langle\tau_\alpha\rangle$ , are reached at higher temperatures in maltitol than in sorbitol. Because the  $\beta$  relaxations in sorbitol and maltitol are superposable, as shown before, this obviously reflects the difference in branching position,  $T_{\alpha\beta}$ , of the most probable times  $\langle\tau_\alpha\rangle$  and  $\langle\tau_\beta\rangle$ . As underlined before, the TSDC technique provides an outlook of the  $\beta$ - $\alpha$  branching, not at the level of the most probable time but in the wings of the time distributions of the two processes.

The presence of the heterocyclic substituent in maltitol leads, on the other hand, to the existence of different types of local intramolecular motions: those in the aliphatic chain, those in the heterocyclic substituent, and those arising from the local cooperative interaction between the aliphatic chain and the heterocyclic substituent. This was clearly shown from the TSDC results where a slight structuration was visible for the  $\beta$  relaxation.<sup>3</sup> In contrast, the TSDC global peak for the  $\beta$  relaxation of sorbitol did not show any apparent structuration (see Figure 3). However, the structural difference between maltitol and sorbitol has no influence on the temperature dependence of the  $\beta$  relaxation time.

Finally, let us briefly comment on the cooperativity of the  $\beta$  relaxation, its spatial uniformity or heterogeneity, and the contribution the TSDC technique can make to the discussion of these problems. Two different scenarios are considered to describe the  $\beta$ -relaxation phenomenology. According to one of these scenarios, the so-called homogeneous picture, each molecule contributes to the secondary process by a small, local librational motion. Each relaxing unit that contributes to the main relaxation also contributes, according to this picture, to the secondary relaxation, but through localized and smaller-amplitude motions. The other scenario, the so-called heterogeneous one, is that of "islands of mobility", proposed by Johari.<sup>19</sup> According to this phenomenological description, microdomains or clusters of molecules survive in the frozen material well below  $T_g$ , and their relaxational behavior is distinct from that of the bulk in that it retains motional degrees of freedom that give rise to the  $\beta$  relaxation. According to this view, the  $\beta$  relaxation would be reminiscent of the  $\alpha$  relaxation on a much smaller scale. In this context, it seems not unreasonable to consider that the  $\beta$  relaxation would show a certain degree of cooperativity, much lower than the cooperativity that characterizes the  $\alpha$  relaxation. Some authors have, in fact, provided

support for a cooperative character of the secondary relaxation,<sup>20,21</sup> arguing that the preexponential factor of the  $\beta$  relaxation determined by dielectric relaxation spectroscopy is often found to be significantly lower than  $\tau_0 \approx 10^{-13}$  s (see Figure 5). However, the TSDC technique unequivocally shows that the TS components of most of the relaxations observed in the glassy state strictly obey the zero-entropy approximation or, stated otherwise, that they show preexponential factors on the order of  $\tau_0 \approx 10^{-13}$  s.<sup>22</sup> This is clearly shown in Figures 5 and 6, and it indicates that the  $\beta$  relaxation in sorbitol arises from local and noncooperative motions. Moreover, this observation can reasonably be considered as an indication of the spatial uniformity of this relaxation, in agreement with recent works by R. Richert.<sup>6,7</sup>

**$\alpha$  Relaxation and Fragility.** Some TS components of the  $\alpha$  relaxation of sorbitol are shown in Figure 7. The TS component with higher intensity is located at  $T_M = -0.7$  °C and was obtained with a polarization temperature of  $T_P = -8$  °C.

It is to be noted that the configurations of the TS peaks in the glass transition region show some features that are indicative of the overlap of the  $\alpha$  and  $\beta$  relaxations. In fact, for systems in which no secondary relaxations exist in the proximity of the  $\alpha$  relaxation, as is the case for salol and glycerol,<sup>3</sup> the locations of the TS peaks in the glass transition region changes over a very narrow temperature range. This is not the case for sorbitol, as shown in Figure 7, where the lower-intensity peaks of the lower-temperature side merge gradually into the glass transition region. As indicated before, this is a consequence of the crossing, or intersection, of the tails of the time distributions of the secondary and primary processes in the TSDC time window. This intersection of the distribution tails, which is well illustrated in Figure 5, is the TSDC image of the  $\beta$ - $\alpha$  branching at  $T_{\alpha\beta}$  of the most probable times.

As reported before and discussed elsewhere,<sup>3,4</sup> the  $\log \tau(T)$  versus  $1/T$  lines of the TS components of the glass transition relaxation exhibit significant curvature, so the activation parameters were obtained at  $T_m$  by fitting the  $\log \tau$  versus  $1/T$  curve with a nonlinear equation. The values of the activation enthalpies of some TS peaks in the glass transition region are presented in Figure 6 as a function of  $T_m$  (the location of the TS peak in the temperature axis). A very strong departure from the zero-entropy prediction can be observed, which is a feature of the glass transition relaxation as studied by TSDC.<sup>3,23</sup>

It was recently suggested<sup>2,3</sup> that the amplitude of the deviation from the zero-entropy prediction provides relevant information concerning the topology of the surface of activation barriers associated with the glass transition relaxation. In this context, a procedure was proposed to evaluate the fragility of a glass from the amplitude of the deviation from the zero-entropy approximation.

The fragility index,  $m$ , of a given substance is defined<sup>24-26</sup> as

$$m = \left[ \frac{d \log_{10} \tau(T)}{d(T_g/T)} \right]_{T=T_g} \quad (1)$$

and corresponds to the slope at  $T_g$  of the representation of  $\log \tau$  versus  $1/T$  divided by  $T_g$ . In this definition,  $\tau$  is the structural relaxation time, which slows down to  $\sim 100$  s at  $T_g$ . The fragility of a material is determined by the topology of its energy landscape or, stated differently, by the amplitude of the energy barriers and their density. Considering the TS peak with higher intensity in the glass transition region, whose location is at  $T_M \approx T_g$ , the activation enthalpy at  $T_M$ ,  $\Delta H^\ddagger(T_M)$ , can be obtained

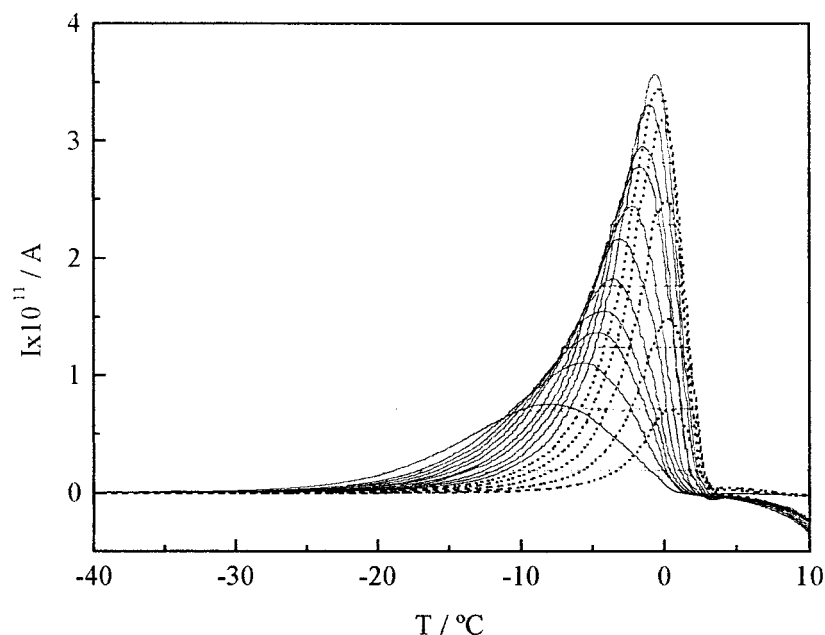


**Figure 7.** TS components of the glass transition relaxation of sorbitol obtained at a heating rate of  $4\text{ }^{\circ}\text{C min}^{-1}$  and with a polarization window of  $2\text{ }^{\circ}\text{C}$ . The polarization temperatures were  $T_p = -20, -17, -16, -15, -14, -13, -12, -11, -10, -9, -8, -7, -6, -5, -4$ , and  $-3\text{ }^{\circ}\text{C}$ . The strength of the polarizing electric field was  $E = 100\text{ V/mm}$ , and the polarization time was 5 min.

**TABLE 1: Glass Transition Temperature,  $T_g$ , and Fragility Index of Some Molecular Glass Formers<sup>a</sup>**

glass former	$T_g$ (K)	$m$	$m_1$	$m_2$
cyano-adamantane	177	35 <sup>25</sup>	20.5 <sup>28</sup>	5.6
glycerol	185	53 <sup>25</sup>	58 <sup>3</sup>	43
<i>m</i> -toluidine	187	79 <sup>26</sup>	83 <sup>4</sup>	69
salol	220	73 <sup>25</sup>	65 <sup>3</sup>	50
sorbitol	272	93, <sup>25</sup> 72 <sup>29</sup>	74	59
maltitol	311	80, <sup>30</sup> 75, <sup>31</sup> 72 <sup>29</sup>	74 <sup>3</sup>	59

<sup>a</sup> Values of  $m$  are taken from the literature, whereas  $m_1$  and  $m_2$  are calculated, respectively, from eqs 2 and 3.

by fitting the corresponding  $\log \tau$  versus  $1/T$  line. We can thus obtain the fragility index from the TSDC data using<sup>27</sup>

$$m_1 = \left[ \frac{d \log_{10} \tau(T)}{d(T_M/T)} \right]_{T=T_M} = \frac{1}{2.303} \left[ 1 + \frac{\Delta H^{\ddagger}(T_M)}{RT_M} \right] \quad (2)$$

It can be seen from Table 1 that the values of the fragility  $m_1$  for sorbitol and other glass formers obtained from the TSDC data using eq 2 are in very reasonable agreement with the literature values obtained from other techniques using eq 1. The obtained results show that, despite the difference in their glass transition temperatures, sorbitol and maltitol have the same fragilities. This arises from the fact that the bulky substituent in maltitol hinders, i.e., increases the activation energy of, the molecular motions associated with the glass transition relaxation, giving rise to a higher amplitude of the deviation from the zero-entropy hypothesis. This is shown in Figure 6 where the full symbols, which correspond to the TS component with higher intensity in the glass transition region, indicate that the activation enthalpy at  $T_M$  is slightly higher in maltitol than in sorbitol.

The fragility scale based on eq 1, and also that based on eq 2, is such that the limit of fragility for infinitely strong glasses is  $m \approx 15\text{--}16$ .<sup>25</sup> This limit arises from the facts that, for thermally activated processes, the Arrhenius preexponential factor is typically such that  $\tau_0 \approx 10^{-13}\text{--}10^{-14}$  and the relaxation time at the glass transition temperature has a characteristic value of  $\tau(T_g) \approx 100\text{ s}$ . Because the essential feature of the glass

transition relaxation is the departure of the activation enthalpy from the zero-entropy prediction, rather than the activation enthalpy at  $T_g$  itself, an absolute scale of fragility based on this concept was proposed (see refs 3 and 4 for further explanation) and defined as

$$m_2 = \frac{\Delta}{2.303 \times RT_M} \quad (3)$$

where  $\Delta$  is the amplitude of the departure from the zero-entropy approximation.<sup>2,3</sup> The values of the fragility  $m_2$  calculated using eq 3 are also presented in Table 1.

## Conclusions

From the results obtained in this TSDC study, we can conclude that the  $\beta$  relaxation in D-sorbitol (or D-glucitol) appears to be strongly overlapped with the  $\alpha$  relaxation in the temperature range between  $-60$  and  $-15\text{ }^{\circ}\text{C}$  and does not show any sign of structuration. This behavior contrasts with that observed for maltitol, a derivative of D-glucitol, where the presence of a bulky heterocyclic substituent separates the motions associated with the secondary and primary relaxations. The map of the most probable relaxation times provided by dielectric relaxation spectroscopy was compared with the map of relaxation times provided by TSDC. It was shown that the  $\alpha$ - $\beta$  branching that occurs at  $T_{\alpha\beta} \approx 335\text{ K}$  in sorbitol (temperature at which the most probable relaxation times of both relaxations are equal) is observed in TSDC under the form of a merging between the higher-temperature TS peaks of the  $\beta$  relaxation and the lower-temperature TS peaks of the  $\alpha$  relaxation, which occurs in the temperature region between  $-60$  and  $-15\text{ }^{\circ}\text{C}$ . The TSDC technique thus provides a perspective on the  $\beta$ - $\alpha$  branching, not at the level of the most probable time but rather in the wings of the time distributions of the two processes.

The TSDC study of the  $\alpha$  relaxation of sorbitol showed, as expected, a strong departure from the zero-entropy approximation. From the amplitude of this departure, a fragility value of  $m = 74$  was obtained, which compares reasonably with the

values reported in the literature and obtained by other techniques. This value is the same as was obtained for maltitol, despite the fact that the glass transition temperature of this glass former ( $T_g = 311$  K) is appreciably higher than that of sorbitol ( $T_g = 271.8$  K).

**Acknowledgment.** N. T. Correia and C. Alvarez acknowledge grants from the Praxis XXI program. Support from a Franco-Portuguese cooperation protocol (ICCTI/French Embassy no. 98/101) is gratefully acknowledged.

## References and Notes

- (1) Correia, N. T.; Moura Ramos, J. J. *J. Polym. Sci. B: Polym. Phys.* **1999**, *37*, 227.
- (2) Alvarez, C.; Correia, N. T.; Moura Ramos, J. J.; Fernandes, A. C. *Polymer* **2000**, *41*, 2907.
- (3) Correia, N. T.; Alvarez, C.; Moura Ramos, J. J.; Descamps, M. *Chem. Phys.* **2000**, *252*, 151.
- (4) Correia, N. T.; Alvarez, C.; Moura Ramos, J. J.; Descamps, M. *J. Chem. Phys.* **2000**, *113*, 3204.
- (5) Faivre, A.; Niquet, G.; Maglione, M.; Fornazero, J.; Jal, J. F.; David, L. *Eur. Phys. J. B* **1999**, *10*, 277.
- (6) Wagner, H.; Richert, R. *J. Phys. Chem. B* **1999**, *103*, 4071.
- (7) Wagner, H.; Richert, R. *J. Non-Cryst. Solids* **1998**, *242*, 19.
- (8) Fujima, T.; Frusaka, H.; Ito, K.; Hayakawa, R. *Jpn. J. Appl. Phys.* **2000**, *39*, L744.
- (9) Siniti, M.; Carré, J.; Letoffé, J. M.; Bastide, J. P.; Claudy, P. *Thermochim. Acta* **1993**, *224*, 97.
- (10) Siniti, M.; Jabrane, S.; Letoffé, J. M. *Thermochim. Acta* **1999**, *325*, 171.
- (11) Correia, N. T.; Campos, J. M.; Moura Ramos, J. J. *J. Chem. Soc., Faraday Trans.* **1997**, *93*, 157.
- (12) van Turnhout, J. *Thermally Stimulated Discharge of Polymer Electrets*; Elsevier: New York, 1975.
- (13) Chen, R.; Kirsch, Y. *Analysis of Thermally Stimulated Processes*; Pergamon Press: New York, 1981.
- (14) The procedure used to calculate the  $\log \tau(T)$  versus  $1/T$  line for a given TS peak is very common for TSDC users. Readers who are not familiar with this technique are recommended to look at ref 3, where this problem is described in some detail.
- (15) Bucci, C.; Fieschi, R.; Guidi, G. *Phys. Rev.* **1966**, *148*, 816.
- (16) Teyssède, G.; Lacabanne, C. *J. Phys. D: Appl. Phys.* **1995**, *23*, 1478.
- (17) Sauer, B. B.; Avakian, P.; Starkweather, H. W.; Hsiao, B. S. *Macromolecules* **1990**, *23*, 5119.
- (18) Gangasharan; Murthy, S. S. N. *J. Phys. Chem.* **1995**, *99*, 12349.
- (19) Cavaillé, J. Y.; Perez, J.; Johari, G. P. *Phys. Rev. B* **1989**, *39*, 2411.
- (20) Ngai, K. L.; Schonhals, A. *J. Polym. Sci. B: Polym. Phys.* **1998**, *36*, 1927.
- (21) Kudlick, A.; Benkhof, S.; Blochowicz, T.; Tschirwitz, C. T.; Rossler, E. *J. Mol. Struct.* **1999**, *479*, 201.
- (22) Correia, N. T.; Moura Ramos, J. J. *Phys. Chem. Chem. Phys.* **2000**, *2*, 5712.
- (23) Moura Ramos, J. J.; Mano, J. F.; Sauer, B. B. *Polymer* **1997**, *38*, 1081.
- (24) Bohmer, R.; Angell, C. A. Local and Global Relaxations in Glass Forming Materials. In *Disorder Effects on Relaxational Processes*; Richert, R., Blumen, A., Eds.; Springer-Verlag: Berlin, 1994.
- (25) Bohmer, R.; Ngai, K. L.; Angell, C. A.; Plazek, D. J. *J. Chem. Phys.* **1993**, *99*, 4201.
- (26) Angell, C. A. *J. Res. Natl. Inst. Stand. Technol.* **1997**, *102*, 171.
- (27) The full explanation of this procedure for obtaining the fragility index from TSDC data has been presented before<sup>2-4</sup> and, for this reason, is not repeated here.
- (28) Moura Ramos, J. J. *Mol. Phys.* **1997**, *90*, 235.
- (29) Carpentier, L.; Descamps, M., to be published.
- (30) Lebrun, N.; Bustin, O.; van Miltenburg, J. C.; Carpentier, L.; Descamps, M. 24<sup>th</sup> *Ames Journées d'Équilibre Entre Phases (JEEP 98)*, Nancy, France, April 1-2, 1998.
- (31) Bustin, O.; Descamps, M. *J. Chem. Phys.* **1999**, *110*, 10982.